Journal of Radiation Research, Vol. 59, No. 5, 2018, pp. 529–540
doi: 10.1093/jrr/rry043
Advance Access Publication: 12 June 2018

Pancreatic radiation effect in apoptosis-related rectal radiation toxicity

Sei Hwan You[1,2], Mee Yon Cho[3], Joon Hyung Sohn[4] and Chang Geol Lee[1,*]

[1]Department of Radiation Oncology, Yonsei University College of Medicine, 50-1 Yonsei-ro, Seodaemun-gu, Seoul 03722, Republic of Korea
[2]Department of Radiation Oncology, Yonsei University Wonju College of Medicine, 20 Ilsan-ro, Wonju 26426, Republic of Korea
[3]Department of Pathology, Yonsei University Wonju College of Medicine, 20 Ilsan-ro, Wonju 26426, Republic of Korea
[4]Institute of Lifestyle Medicine, Yonsei University Wonju College of Medicine, 20 Ilsan-ro, Wonju 26426, Republic of Korea
*Corresponding author. Department of Radiation Oncology, Yonsei University College of Medicine, 50-1 Yonsei-ro, Seodaemun-gu, Seoul 03722, Republic of Korea. Tel: +82-2-2228-8095; Fax: +82-2-2227-7823; Email: cglee1023@yuhs.ac
(Received 7 January 2018; revised 19 March 2018; editorial decision 25 April 2018)

ABSTRACT

Pancreatic radiation effect (PRE) can be a component of gastrointestinal tract (GIT) radiotoxicity. This inter-organ correlation between the GIT and the pancreas was assessed through a rat model. Separate local irradiation to the abdomen and the pelvis was applied concurrently for 8-week-old male Sprague Dawley rats. Abdominal irradiation was categorized into pancreatic shield (PS) and non-pancreatic shield (NPS) irradiation. After 5 Gy and 15 Gy irradiation, the rectal mucosa was analyzed at the first week (early phase, Ep) and the 14th week (late phase, Lp). A slow gain in body weight was observed initially, particularly in the NPS group receiving a 15 Gy dose ($P < 0.001$). The large number of apoptotic bodies after 15 Gy at Ep decreased at Lp. At Ep for the 5-Gy group, the NPS group revealed more fibrotic change than the PS group ($P = 0.002$). Cleaved caspase-3 (CCP3) expression was greater at Lp, and the Ep–Lp increase was prominent in the NPS-15-Gy group ($P = 0.010$). At Lp, for 15 Gy irradiation, CCP3 was expressed more in the NPS group than in the PS group ($P = 0.032$). Despite no direct toxicity difference between the PS and NPS groups, small changes in parameters such as fibrosis or CCP3 expression suggest that pancreatic shielding does have an effect on the radiation response in the rectal mucosa, which suggests a need for a multi-organ effect-based approach in GIT radiotoxicity assessment.

Keywords: radiation injuries; gastrointestinal tract; pancreas; nutritional status

INTRODUCTION

The gastrointestinal tract (GIT) is the dose-limiting organ during radiotherapy. Insufficient nutrition, caused by GIT toxicity, slows down tissue recovery, which in turn slows down recovery of the absorption of nutrients. One of the main factors related to GIT toxicity is the degree of mucosal damage, which is caused by loss of balance between damage and regeneration. Apoptosis and clonogenic cell death can lead to cytokine-activated inflammatory reactions with peripheral immune cell activation, depending on the degree of injury [1–4]. However, clinical manifestations cannot always be explained by these mechanisms. The tolerably administered dose for thoracic or pelvic GIT is ~55 Gy, with 1.8–2.0 Gy daily fractions, while it is <50 Gy for upper abdominal GIT [5, 6].

This radiation vulnerability can be explained by the presence of the pancreas, located at the center of the upper abdomen [7–11]. From this perspective, pancreatic radiation effect (PRE) needs to be considered in terms of inter-organ interaction. The purpose of this study was to analyze the GIT radiotoxicity associated with PRE in a rat model. First, we examined the validity of the animal model through an experimentally devised shielding system. Subsequently, rectal radiotoxicity was analyzed to confirm the concept of multisystem dysfunction between the pancreas and rectum.

MATERIALS AND METHODS

Animal preparation

Eight-week-old male Sprague Dawley rats (Daehan Biolink, Eumseong, Korea) were housed with drinking water, a standard 5L79 diet (PMI Inc., St Louis, MO), control of the temperature and humidity, and a 12-h light–dark cycle. Irradiation was performed on the 7th day of the adaptation period post-arrival. The

average body weight at irradiation was 250.9 ± 8.4 g. The status of rats was assessed by veterinarians, and all animal experiments proceeded after approval by the Institutional Animal Care and Use Committee (Approval number: OOO-150519-2).

Irradiation outline

X-rays of 6 MV were delivered using a linear accelerator (Elekta Synergy, Elekta, Stockholm, Sweden). Three-dimensional planning was performed using a computed tomography (CT) (Aquillion LB, TSX-201A, Toshiba Medical Systems Corporation, Otawara, Japan) scan. The beam was delivered by a postero–anterior (PA) and antero–posterior (AP) combination in the prone position on the platform after the posture was set as straight from the neck vertebrae to the tail. The dose rate was 3.6 Gy/min. During CT scanning and irradiation, each rat was anesthetized via isoflurane inhalation using a Small Animal Single Flow (O_2) Anesthesia System (L-PAS-01, LMSKOREA Inc., Seongnam, Korea) with thorough monitoring. The rat position remained stable without a fixation device.

Irradiation in concurrence to pancreas and rectum

The experimental technique of irradiation in concurrence to pancreas and rectum (iCPR) was devised to directly investigate whether rectal toxicity was associated with PRE. Overall, the iCPR volume included both the upper abdomen and the lower pelvis area. Figure 1A indicates schematic beam irradiation before shield application. During the actual irradiation, a specially designed Cerrobend shield system was applied to the upper abdominal area in order to reflect PRE, and we distinguished into the pancreatic shield (PS) (Fig. 1B) and non-pancreatic shield (NPS) (Fig. 1C) groups by the shape of the shield block. A constant pelvic radiation field was maintained to ensure a fixed rectal dose as the main object of toxicity analysis.

Irradiation planning

Following CT scan (2 mm-sliced), the major abdominal organs (liver, stomach, bilateral kidneys, and pancreas) were delineated using the Pinnacle3 planning system (Philips Healthcare, Andover, MA) (Fig. 2A). The central part of the pancreas was contoured from the level of the renal upper pole to eight slices upwards. The pelvic contour was delineated from the anal verge to the 18th slice upward, encompassing the whole rectum. The abdomino–pelvic contour, as a substitute for the whole body, was delineated from the diaphragm to the anal verge level. The thorax was excluded due to its small volumetric impact. The NPS was set to a circular shape by homogeneous pancreatic contour expansion. The PS was derived as a ring-shaped structure by additional expansion of the NPS margin (Fig. 2B). The lower pelvic field was fixed to a 3.4 cm × 3.6 cm-sized open rectangular shape and the whole portal area was 3.4 cm × 12.0 cm. The irradiation dose in planning was 5 Gy and 15 Gy with single

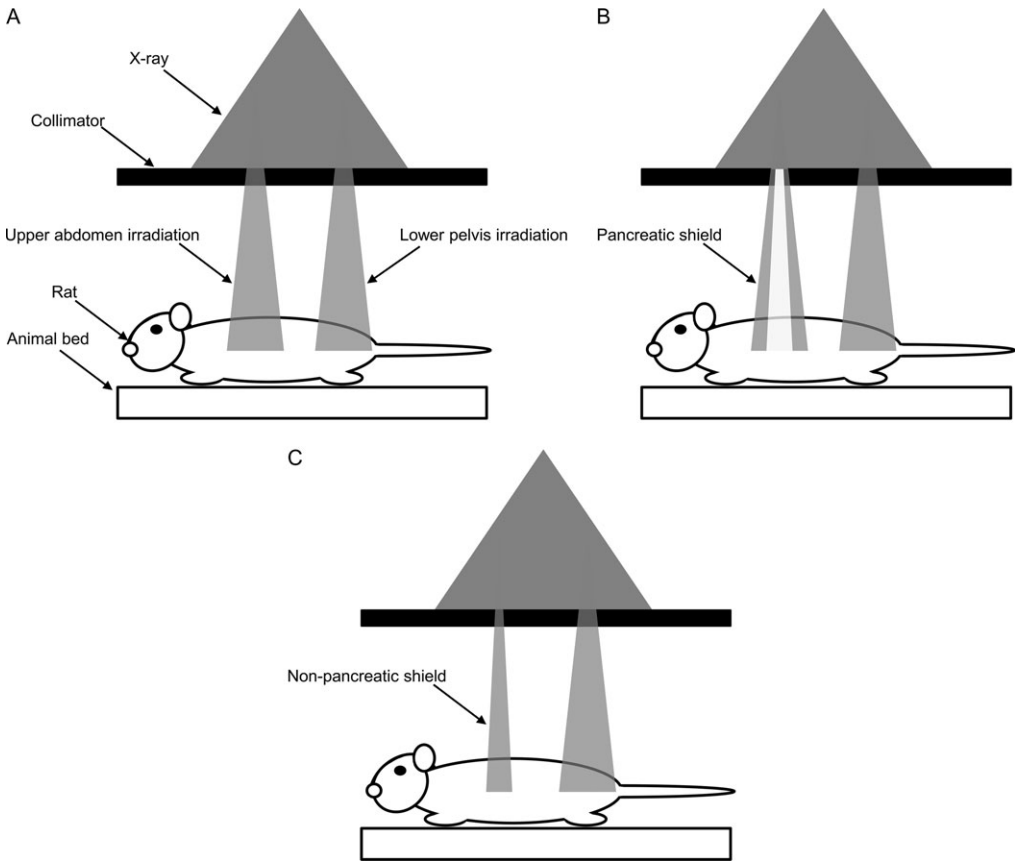

Fig. 1. Schematic diagrams of rat irradiation method. (A) Irradiation in concurrence to pancreas and rectum (iCPR) without shield. (B) iCPR with pancreatic shield. (C) iCPR with non-pancreatic shield.

fractionation, in the low- and high-dose groups, respectively. Thus, the estimated dose to the rectum was 5 Gy and 15 Gy in the low- and high-dose group, respectively. In the PS groups, the central dose to the pancreas was 0 Gy. In the 5 Gy-NPS and 15 Gy-NPS groups, the central dose to the pancreas was 5 Gy and 15 Gy, respectively. After dosimetric estimation for seven sample rats, the standardized prescription location (mid-depth point of the upward 7th slice from the pelvic contour upper margin) and monitor unit values for PA/AP portals (280/275 for 5 Gy and 840/825 for 15 Gy) were derived. These conditions were applied to the irradiation for rectal radiotoxicity analysis (Fig. 2C).

Validation

Gafchromic EBT3 film (Ashland, Bridgewater, NJ) dosimetry was performed with a solid water phantom (RW3 Slab Phantom, PTW, Freiburg, Germany) and an ion chamber (TM 30013, PTW, Freiburg, Germany). The 6-MV X-ray beam was delivered perpendicularly to the film with the following conditions: 2-cm depth, 3.6-Gy/min dose rate, and 17-cm source-to-surface distance. The iCPR was applied with 5 Gy irradiation followed by dose profile confirmation for both PS and NPS (Fig. 2D).

Body weight and blood glucose measurement

Blood glucose level and body weight were measured at 0, 1, 5, 9 and 14 weeks after irradiation. Blood glucose was measured in rat tail vessel blood, using a measurement kit (Accu-CHEK, Roche Diabetes Care GmbH, Mannheim, Germany), with overnight fasting (18 h).

Tissue extraction

Rats were sacrificed at the end of the first week (early phase, Ep) and end of the 14th week (late phase, Lp) after irradiation. The rectum was excised from the area where the colon exits out of the peritoneum into the anal area. The length before excision was ~3.5 cm,

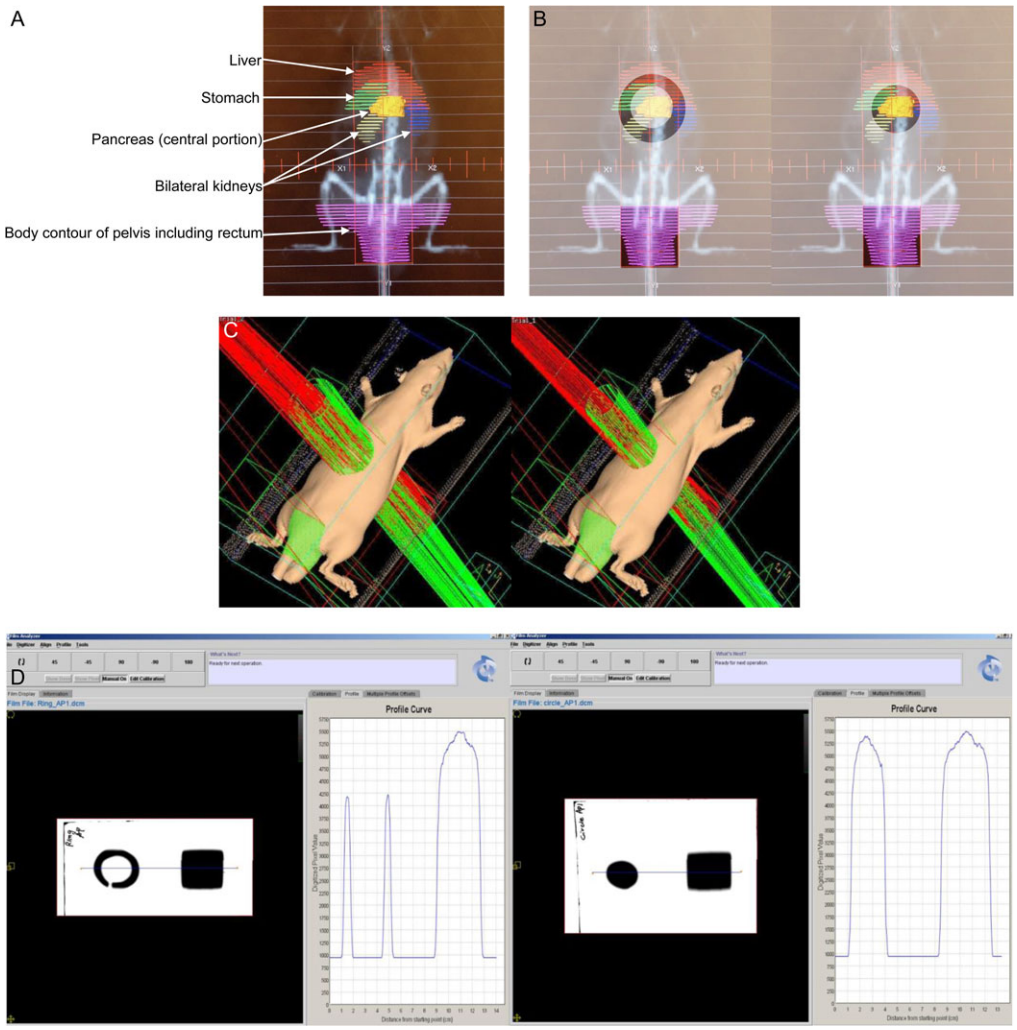

Fig. 2. An example of a pancreatic shield and radiation planning process using a technique of irradiation in concurrence to pancreas and rectum (iCPR). (A) Postero–anterior beam's eye view with contoured organs. (B) Actual radiation exposure after shield system application; pancreatic shield (PS, left) and non-pancreatic shield (NPS, right). (C) Rendered images of radiation planning for PS irradiation (left) and NPS irradiation (right) for postero–anterior/antero–posterior portals. (D) Dose profiles of PS (left) and NPS (right) applied to solid water phantom.

which was matched by the length of the longitudinal axis of the lower pelvic field. The specimens were fixed in phosphate-buffered 10% formalin and axially sectioned at the mid-point for paraffin embedding.

Hematoxylin and eosin staining

Hematoxylin and eosin (HE) staining was performed on paraffin-embedded tissue sections. Apoptotic bodies were counted in the entire mucosal villi of a longitudinal shape on the cross section at ×400 magnification. The number of apoptotic bodies per 100 crypts was defined as the apoptotic index (AI). Morphological guidelines were as per previous representative studies [12, 13].

Picrosirius red staining

The degree of fibrotic change was estimated by the proportion of fibrosis in the mucosal layer. The tissue section was stained by a Picrosirius red (PR) kit (Polysciences, Inc., Warrington, PA) using the single uniform red-based staining property contrasted with the unstained glandular areas. The PR-positive proportion (PR positivity) was quantitated using a computerized imaging tool (NIS-Elements BR version 4.30, Nikon Instruments Inc., Melville, NY) with consistent intensity for each ×100 magnification image.

Table 1. Group classification for male Sprague Dawley rats and their number allocation according to radiation dose, pancreatic shielding, and time phase after irradiation

Group category	Pancreatic shield	Non-pancreatic shield
Early phase (1 week after irradiation)		
5 Gy	6	6
15 Gy	6	6
Late phase (14 weeks after irradiation)		
5 Gy	6	6
15 Gy	6	6

Immunohistochemical staining

The degree of apoptotic activity was estimated by immunohistochemical (IHC) staining for cleaved caspase-3 (CCP3) in the mucosal layer. Following section deparaffinization and an an antigen-retrieval for 60 min, endogenous peroxidase activity was blocked by exposing the sections to an ultraviolet inhibitor for 4 min. After the reaction buffer washing, an Ultra View Universal DAB Detection Kit (Ventana Medical Systems, Tucson, AZ) was used for IHC staining. The slides were incubated with monoclonal antibodies against CCP3 (1:100, #9664, Cell Signaling Technology, Inc., Danvers, MA) for 1 h at 37°C in an autostainer (Benchmark XT, Ventana Medical Systems) and rinsed with the reaction buffer. Drops of the following reagents were applied sequentially to each slide (8 min per reagent), and rinsed again with reaction buffer: HRP UNIV MULT, DAB H_2O_2 and COPPER (Ventana Medical Systems). The slides were subsequently treated with hematoxylin for 4 min, incubated with bluing reagent for 4 min, and finally rinsed with reaction buffer. Negative control sections were also processed to evaluate for the specificity of primary antibody or background staining levels. CCP3-positive cells were counted in the representative mucosal area on the cross-section at ×400 magnification. The number of CCP3-positive cells per 100 epithelial cells in the crypts was defined as the CCP3 positivity.

Table 2. Dosimetric comparison of mean doses of each contour volume for pancreatic shield (PS) and non-pancreatic shield (NPS) groups in seven sample rats, with a 500-cGy prescription using postero–anterior/antero–posterior X-rays

	Volume (ml)[a]	Mean dose (cGy)[a]		*P* value[b]
		Pancreatic shield group	Non-pancreatic shield group	
Liver	8.51 ± 0.62	163.94 ± 16.60	135.37 ± 21.89	0.018
Stomach	3.78 ± 0.55	146.03 ± 32.82	95.96 ± 19.11	0.004
Right kidney	1.32 ± 0.13	127.87 ± 38.07	96.17 ± 39.33	0.151
Left kidney	1.22 ± 0.13	93.16 ± 21.77	38.94 ± 15.51	<0.001
Pelvic contour[c]	36.93 ± 3.74	265.33 ± 15.76	264.29 ± 16.11	0.905
Abdomino–pelvic contour[d]	171.43 ± 8.74	103.59 ± 4.20	106.23 ± 4.27	0.265
Pancreas	1.86 ± 0.23	53.33 ± 9.90	464.04 ± 8.37	<0.001

[a]The values are shown as the mean ± standard error.
[b]Student *t* test for mean doses of each contour volume, between the pancreatic shield and the non-pancreatic shield groups.
[c]The pelvic contour, including all pelvic organs and skin area, was delineated from the anal verge to the 18th slice location upward, with a 2-mm thickness.
[d]The abdomino–pelvic contour was delineated from the diaphragm to the anal verge level for integral dose assessment, as a substitute for the whole body, reflecting the radiosensitive gastrointestinal area.

Quantification of mRNAs for inflammation-related proteins

For quantitative polymerase chain reaction (qPCR) analysis, tissue samples were acquired from the area adjacent to the rectal longitudinal mid-point. Samples were rinsed with normal saline and stored at −80°C. RNA was extracted using the RNeasy mini kit (Qiagen, Hilden, Germany) according to the manufacturer's instructions. The reverse transcription reaction was performed with 100 ng of total RNA using the ReverTra Ace® qPCR RT Master Mix with gDNA Remover (Toyobo, Osaka, Japan). Amplification of cytokine genes and 18s RNA was monitored and analyzed using the PowerUp™ SYBR Green Master Mix (Thermo Fisher Scientific Inc., Waltham, MA) and the 7900HT Real-Time PCR System (Thermo Fisher Scientific Inc.). The following primers were used: interleukin-6 (IL-6) (Rn_Il6_1_SG QuantiTect Primer Assay, Qiagen), nuclear factor (NF)-κB (Rn_Nfkb1_1_SG QuantiTect Primer Assay), hypoxia-inducible factor (HIF)-1α (Rn_Hif1a_1_SG QuantiTect Primer Assay), vascular endothelial growth factor (VEGF)-A (Rn_RGD:619991_1_SG QuantiTect Primer Assay), and of the endogenous control gene 18s RNA (Rn_Rn18s_1_SG QuantiTect Primer Assay). PCR amplification was carried out through 10 µl reactions, and at least three replicates were used for each sample. Cycling parameters: 95°C for 10 min, followed by 45 cycles of 95°C for 15 s and 60°C for 60 s. Single product generation was confirmed with a melting curve analysis. Calculations of relative gene expression levels were performed using the $2^{-\Delta\Delta Ct}$ method, by normalizing them to 18s RNA expression levels. A non-irradiated 8-week-old male Sprague Dawley rat was used as a control object. Its rectum tissue was extracted by the same method as for the irradiated groups on the seventh day of the adaptation period post-arrival.

Statistical analysis

The dosimetric comparison of the irradiation planning for the PS group and the NPS group was performed by Student's *t*-test. The parameters of comparison were as follows: body weight, blood glucose, AI, PR positivity, CCP3 positivity, mRNA expression according to dose (5 Gy versus 15 Gy), pancreatic shielding (PS versus NPS), and elapsed time (Ep versus Lp). For multiple comparisons, data were assessed by One-way ANOVA. In each case, Bonferroni's method was chosen for the *post hoc* test to calculate *P*-values for the significance of differences between groups. Analyses were conducted using SPSS version 23 (IBM, Armonk, NY). A $P < 0.05$ was defined as significant. For statistical analysis, six rats were allocated to each group (Table 1).

RESULTS

Sample dosimetry of irradiation technique

According to the mean doses for each contour volume, PS showed higher or equal dose distribution compared with NPS, except for the pancreas. Pelvic and abdomino–pelvic contours did not show a mean dose difference between the PS and NPS groups (Table 2).

Nutrition status and body weight

After irradiation, the body weight gain slowed down at Ep. For the NPS-15-Gy group, it was even reduced temporarily, leading to a significant gap compared with that of the NPS-5 Gy-group ($P < 0.001$, filled stars in Fig. 3A). From the fifth week, the difference in body weight rapidly increased. With the passage of time, the dose-dependent difference in body weight was shifted from the NPS group to the PS group: at the ninth week ($P = 0.035$, empty stars in Fig. 3A) and at Lp ($P = 0.046$, filled circles in Fig. 3A). The blood glucose level decreased markedly at Ep and it recovered gradually after that.

Apoptotic index

By Ep, the number of apoptotic bodies had increased with few inflammatory cell infiltrations, especially in the 15-Gy group

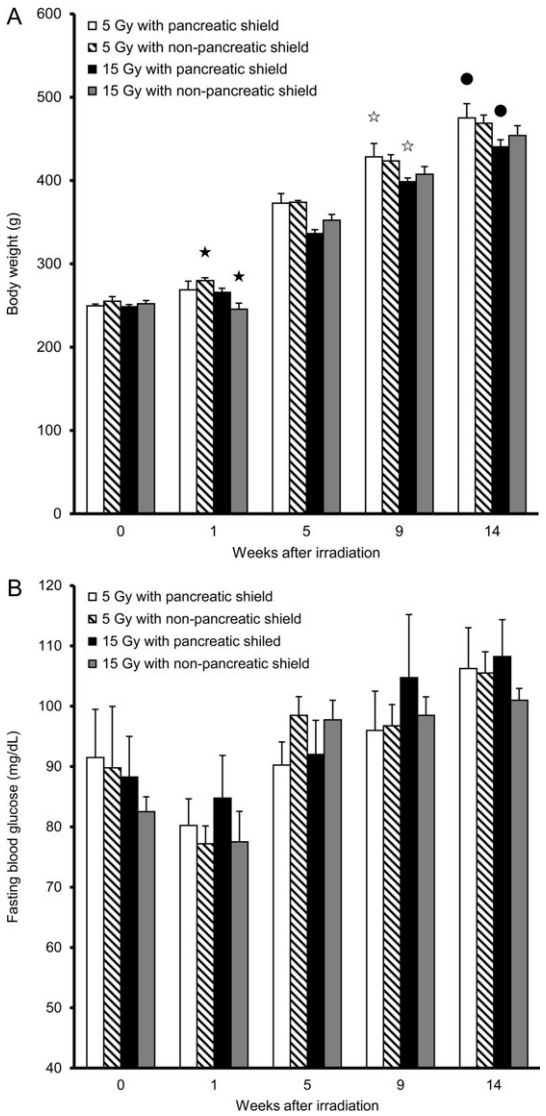

Fig. 3. Changes in body weight (A) and fasting blood glucose (B) after irradiation. Data represent the mean and 95% confidence interval with six samples. Pairs of filled stars, empty stars and filled circles: $P < 0.05$.

(Fig. 4). By Lp, clear indications of recovery were observed. The AI of the PS-5-Gy, NPS-5-Gy, PS-15-Gy and NPS-15-Gy groups at Ep was 41.3 ± 11.0, 47.2 ± 7.4, 127.8 ± 24.9 and 146.0 ± 29.8, respectively. By Lp, the AI had decreased to 28.5 ± 8.2, 32.5 ± 10.2, 50.0 ± 6.3 and 70.0 ± 8.0 in the same groups, respectively. In terms of the PRE, the AI tended to be high in the NPS groups relative to the PS groups, although there was no statistical significance.

Picrosirius red positivity

At Ep, PR positivity of the PS-5-Gy, NPS-5-Gy, PS-15-Gy and NPS-15-Gy groups was 26.12 ± 2.79%, 31.80 ± 1.95%, 34.03 ± 3.06% and 37.87 ± 7.75%, respectively. At Lp, each value tended to converge on ~37% (37.27 ± 2.26%, 37.44 ± 2.56%, 35.05 ± 2.79% and 36.45 ± 5.22% for the same groups) (Fig. 5). A dose-dependent increase was shown in the PS-Ep group ($P = 0.032$, filled stars in Fig. 5I). An increase in PR positivity over time

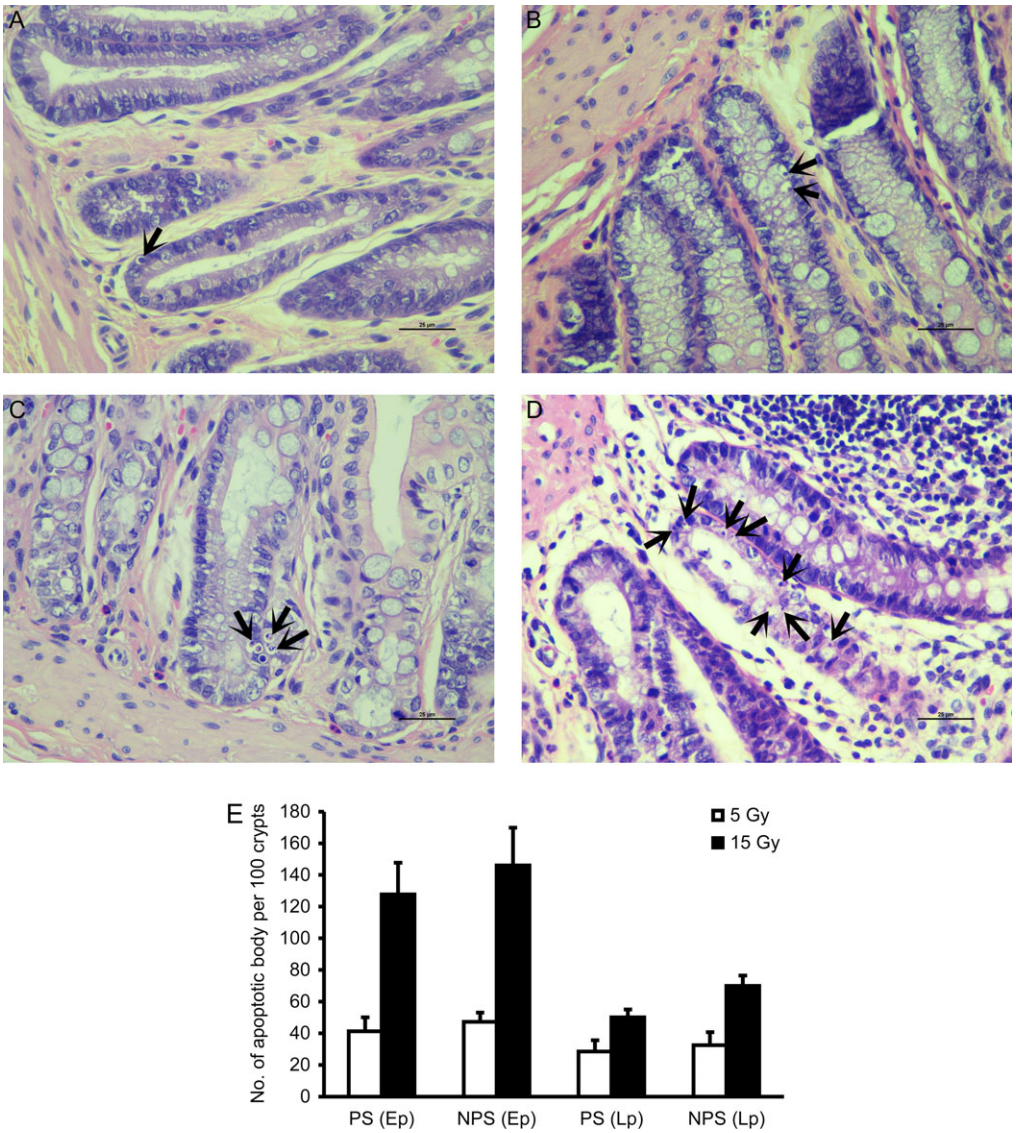

Fig. 4. Apoptosis in rectal mucosa by hematoxylin–eosin stain. (A) to (D) Representative images of axial rectum tissue at the first week (early phase, Ep) after irradiation are shown for pancreatic shield (PS)-5-Gy (A), non-pancreatic shield (NPS)-5-Gy (B), PS-15-Gy (C), and NPS-15-Gy (D) groups. Black arrows, apoptotic bodies in the mucosa. Magnification, ×400. Scale bar, 25 μm. (E) Apoptotic index calculated by the number of apoptotic bodies per 100 crypts on axial rectal mucosa. The images at the 14th week (late phase, Lp) were not displayed due to relatively rare apoptotic bodies with unclear differences for each group. Data represent the mean and 95% confidence interval with six samples.

occurred only in the 5-Gy groups ($P < 0.001$, empty stars and $P = 0.002$, filled circles in Fig. 5I), leading to no significant differences between groups at Lp. It is noteworthy that the PS group showed less PR positivity than the NPS group did at Ep, after 5 Gy irradiation ($P = 0.002$, empty circles in Fig. 5I).

Cleaved caspase-3 positivity

At Ep, CCP3 positivity of the PS-5-Gy, NPS-5-Gy, PS-15-Gy and NPS-15-Gy groups was 1.30 ± 1.06, 1.11 ± 0.47, 2.58 ± 0.81 and 2.95 ± 1.67, respectively. At Lp, each value tended to increase to 2.55 ± 0.94, 2.90 ± 1.99, 3.73 ± 1.02 and 5.59 ± 1.39 for the same

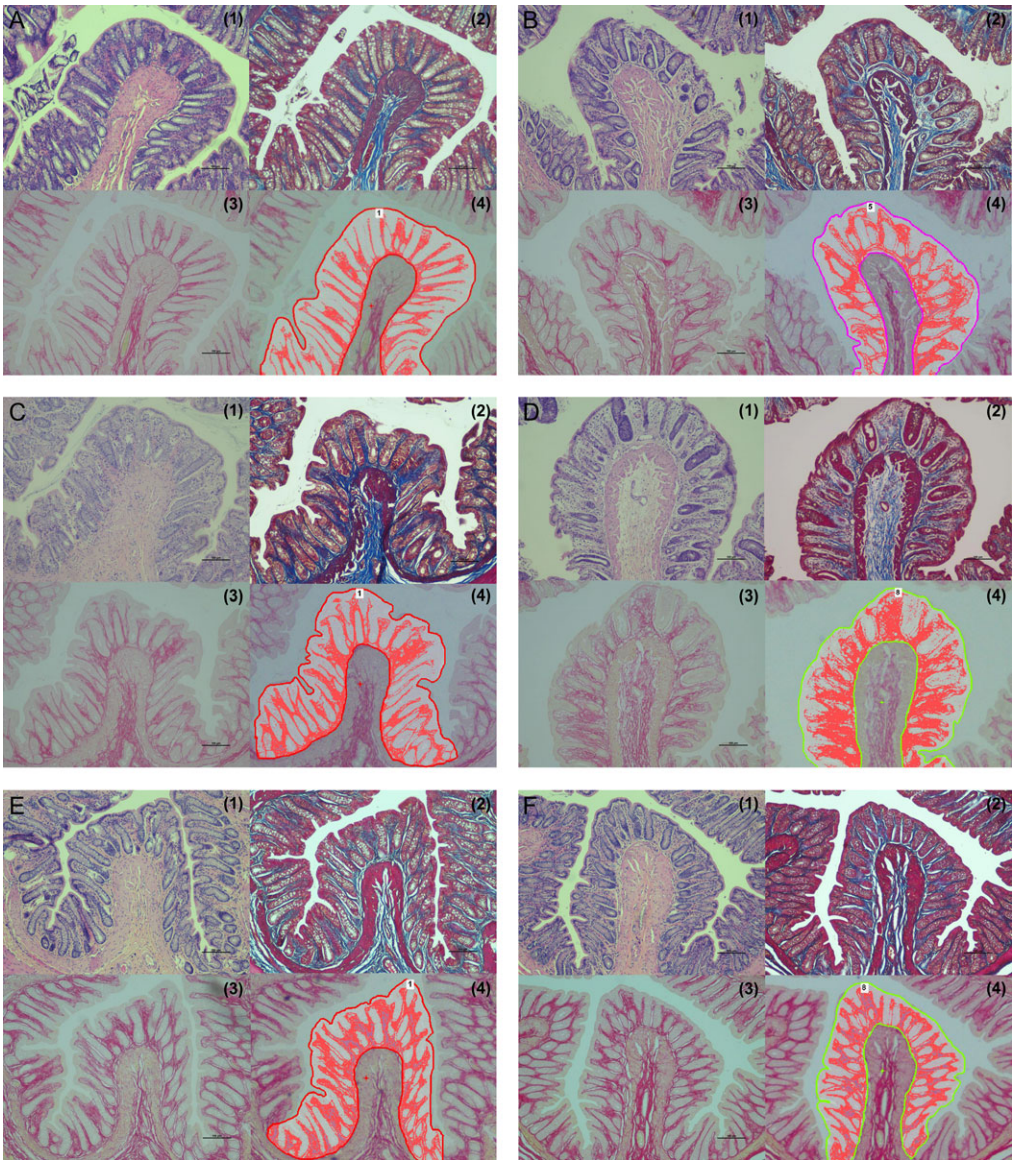

Fig. 5. Fibrotic changes in rectal mucosa by Picrosirius red (PR) staining. Representative images of the axial rectum tissue stained by hematoxylin–eosin (1), Masson's trichrome (2), PR (3), and PR-stained area in a defined range of the mucosal layer (4) are shown for each group at the first week (early phase, Ep) and the 14th week (late phase, Lp). (A) Pancreatic shield (PS)-5-Gy-Ep group. (B) Non-pancreatic shield (NPS)-5-Gy-Ep group. (C) PS-15-Gy-Ep group. (D) NPS-15-Gy-Ep group. (E) PS-5-Gy-Lp group. (F) NPS-5-Gy-Lp group. (G) PS-15-Gy-Lp group. (H) NPS-15-Gy-Lp group. Magnification, ×100. Scale bar, 100 μm. (I) PR positivity calculated quantitatively. Data represent the mean and 95% confidence interval with six samples. Pairs of filled stars, empty stars, filled circles and empty circles: $P < 0.05$.

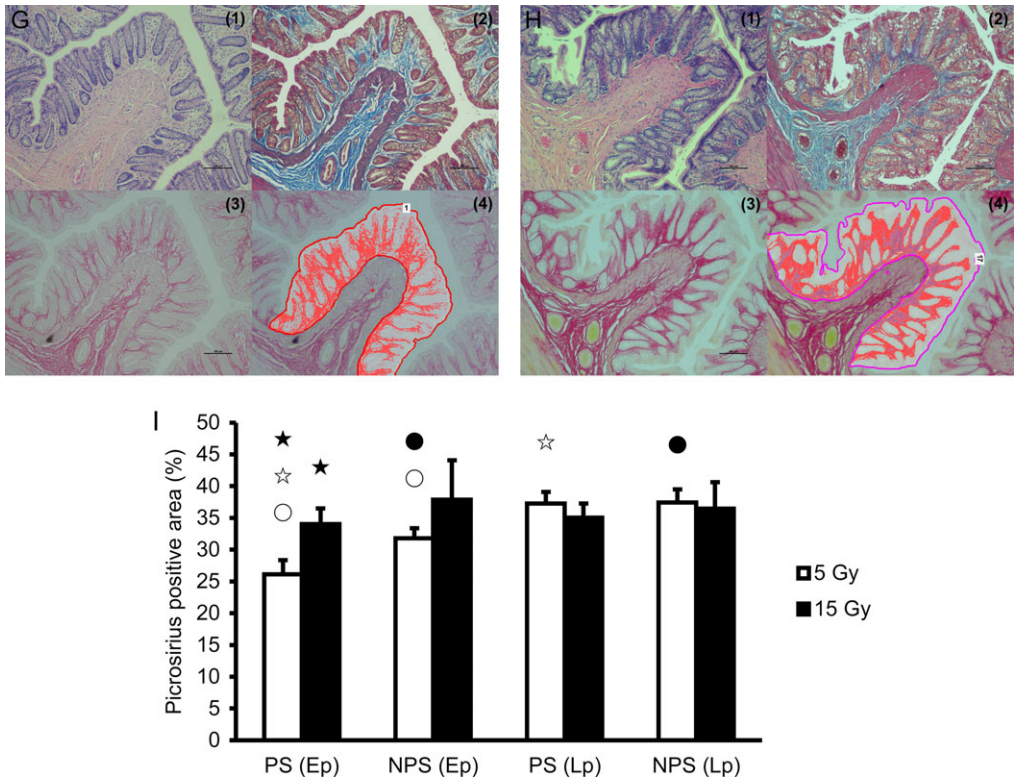

Fig. 5. *Continued*

groups (Fig. 6). This time-dependent increase was significant, especially in the NPS-15-Gy group ($P = 0.010$, filled stars in Fig. 6I). In terms of PRE, CCP3 positivity tended to be higher in the NPS groups relative to the PS groups, especially in the 15-Gy group at Lp ($P = 0.032$, empty stars in Fig. 6I).

mRNA expression

In HIF-1α, VEGF-A and NF-κB, the expressions at Lp tended to be less than those at Ep, with the same dose or PRE status. HIF-1α (three pairs) had the greatest number of significant Ep–Lp decrease pairs (Fig. 7).

DISCUSSION

The radiotoxicity of one organ can be influenced by the status of simultaneously irradiated adjacent other organs [7, 8, 14]. PRE can contribute to GIT toxicity [8, 10]. However, there have not been sufficient follow-up studies investigating this due to the technical difficulty in separately irradiating each organ in the abdomen.

Because of the anatomical location of the pancreas, it is challenging to irradiate the upper GIT while avoiding exposure of the pancreas to radiation. Therefore, it is difficult to examine the effects of pancreatic radiation on radiation damage in the upper GIT. In addition, GIT toxicity can be aggravated by the proteolytic activity of the pancreatic enzymes [15–17]. The rectum, which is free from pancreatic enzyme influence and located far from the pancreas, was estimated to be a valid organ for assessing the PRE in GIT radiotoxicity. The iCPR method allowed for objectivity by targeting the pancreatic enzyme–independent rectum, as an alternative option to the pancreatic enzyme–dependent upper GIT. The PRE-unaffected dose balance is another issue. Our dosimetric comparison between the PS and the NPS showed the feasibility of maintaining the radiation exposure volume in the area around the pancreas, regardless of PRE.

Previous studies showed >25 Gy was required to induce rodent GIT inflammation [18, 19]. This dose level may trigger secondary reactions, making it difficult to establish a GIT toxicity model that reflects the clinical situation. Difficulties are more pronounced in pancreatic histologic change–related cases because the pancreatic radioresistance is much higher [7, 20]. In addition, the dose level of pancreatic histologic injury can result in the problem of unfair assessment originating from a fundamental radiosensitivity difference between the GIT and the pancreas. Our apoptosis-dominant dose level of 5–15 Gy was derived from seeking primary GIT toxicity without inflammatory reactions.

As expected in our study, there was no difference between groups in the microstructure of the pancreas due to the histologic radioresistance (data not shown). However, a relatively low-level effect to the pancreas may disturb the systemic nutritional status. According to Sarri *et al.* [21], 10 Gy irradiation to the entire rat abdomen resulted in rapid normoinsulinemic hypoglycemia without definitive pancreatic histologic change, which may imply impaired

insulin secretion from the islet cells. This hypothesis was applied in our study, and PRE-related malnutrition may have influenced histologic changes in the rectal mucosa.

The value of the serum amylase/lipase was measured in our study. However, there were no differences between the experimental groups (data not shown). There may have been undetected histological damage to the pancreas. Moreover, radiation injury in the GIT may have affected the serum data. On CT-based simulation, the dose exposure to the liver, stomach and left kidney was relatively high in the PS irradiation group compared with that in the NPS group, even under well-balanced irradiation conditions (Table 2). Despite the relatively low dose exposure to the liver, stomach and left kidney in the NPS irradiation group compared with the PS group, histological changes in the NPS group showed a similar or more severe pattern in apoptosis and fibrosis compared with those in the PS group, which indicates the validity of pancreatic dose differentiation by the iCPR method. A recent clinical study revealed possible compromised serum amylase/lipase profiles due to radiation. However, it may not be possible to generalize those results, since the data in that study was confined to the amylase/

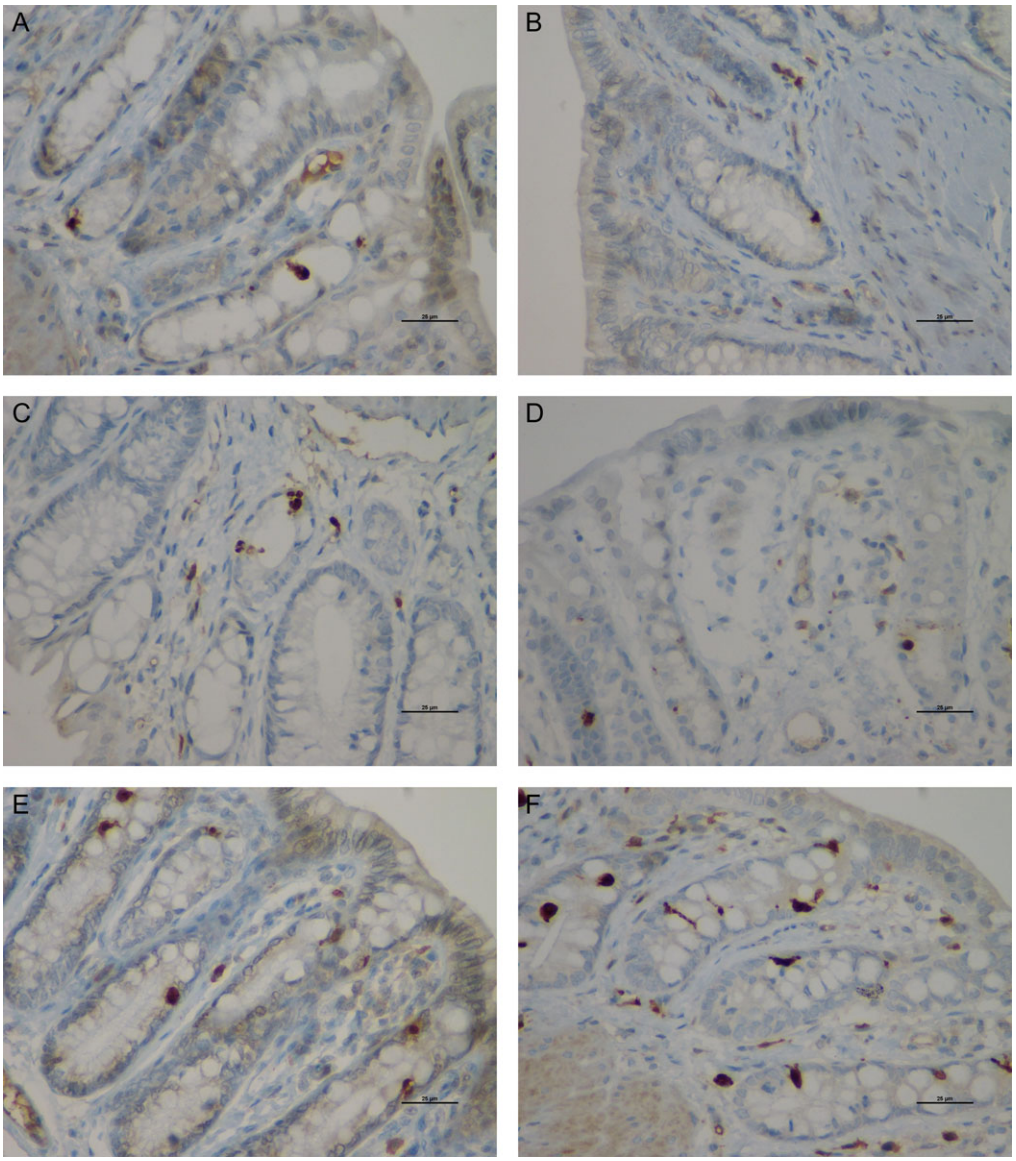

Fig. 6. Cleaved caspase-3 (CCP3)–positive cells by immunohistochemical staining. Representative images of the axial rectum tissue are shown for each group at the first week (early phase, Ep) and the 14th week (late phase, Lp). (A) Pancreatic shield (PS)-5-Gy-Ep group. (B) Non-pancreatic shield (NPS)-5-Gy-Ep group. (C) PS-15-Gy-Ep group. (D) NPS-15-Gy-Ep group. (E) PS-5-Gy-Lp group. (F) NPS-5-Gy-Lp group. (G) PS-15-Gy-Lp group. (H) NPS-15-Gy-Lp group. Magnification, ×400. Scale bar, 25 μm. (I) CCP3 positivity defined as the number of CCP3-positive cells per 100 epithelial cells in the crypts. Data represent the mean and 95% confidence interval with six samples. Pairs of filled stars and empty stars: $P < 0.05$.

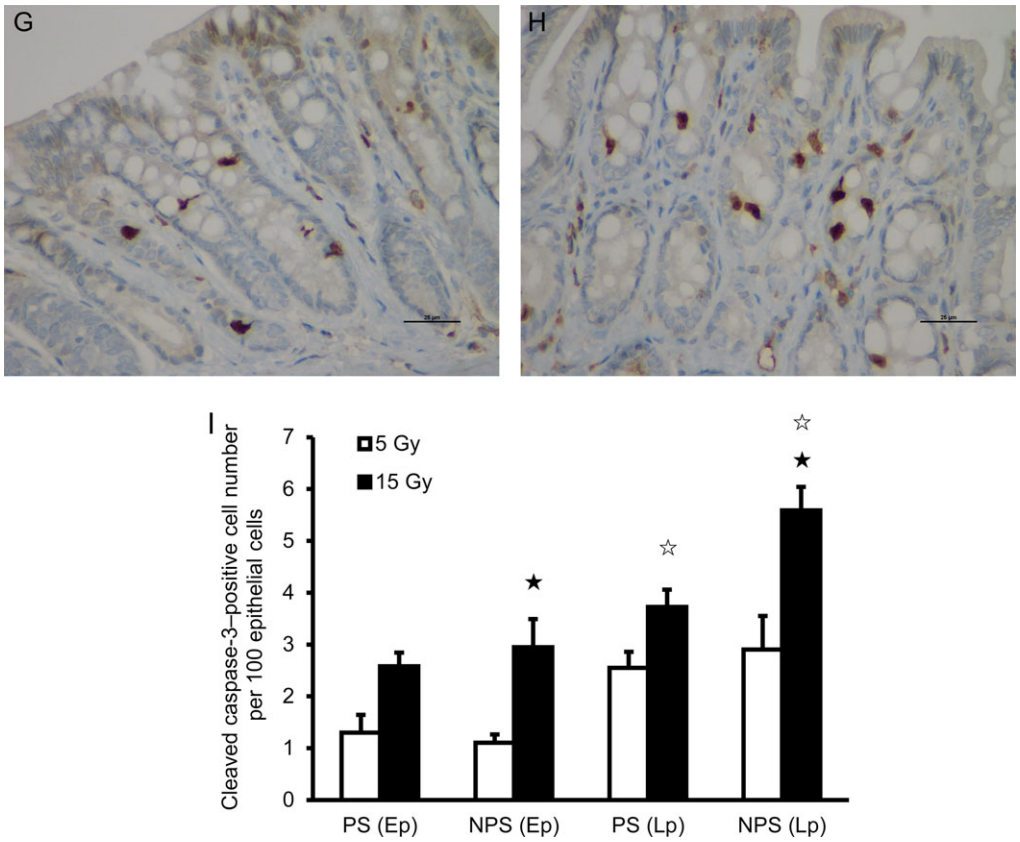

Fig. 6. *Continued*

lipase profiles, and the radiation dose distributions in the abdominal organs were not specified at all [11]. Consequently, at this time, the most reliable parameter for PRE is dosimetric data.

With respect to body weight profile, there seemed to be a dose dependency in the NPS irradiation group at Ep (Fig. 3A). Blood glucose levels were non-specific to PRE, and there was no sign of diabetes (Fig. 3B). This seems to be due to the fact that our radiation dose level was not enough to affect the islet cells. Although there was no direct difference in body weight or blood glucose levels between the PS and NPS group, the changing patterns in body weight according to radiation dose level indicated that there were differences to some extent. This pattern was slightly similar to the apoptotic body–related effects in HE staining. The relatively severe toxicity of the NPS group in the strict comparative conditions of the same rectal radiation dose may represent the PRE impact on the rectal mucosa during its dose-dependent and time course–related trend from Ep to Lp.

The convergence of PR positivity at Lp for all groups may be explained by the increase in 5-Gy (low dose) groups from Ep to Lp (Fig. 5I). In a previous study of a similar situation, there was an overall increase in fibrotic changes, not only in the case of high radiation dose but also with longer post-radiation follow-up time [22]. Fibrosis is known to occur even with acceptably low doses [20], and it was more prominent in the NPS group (Fig. 5I). This PRE-related GIT toxicity pattern was also confirmed for CCP3 positivity, especially in the 15-Gy-Lp group (Fig. 6I). Interestingly, apoptosis-related responses showed a conflicting time-dependent profile according to the analyzing methods. The AI by HE staining increased at Ep and decreased sharply at Lp, especially in the 15 Gy irradiation groups. On the other hand, CCP3 positivity showed a continuous increase until Lp. In the pathways of apoptosis, apoptotic bodies and CCP3 activation seem to be different from each other. This difference may be caused by changes in gut bacteria, intestinal immune environment, or other CCP3-associated tissue responses in the cell death regulation system, and should be explained through further studies [23, 24]. Even though a histologic inflammatory reaction was not apparent, differential expression of inflammation-related mRNA expression was observed. The mRNA expression of HIF-1α, NF-κB and VEGF-A tended to increase at Ep, and tended to decrease by Lp. This might be related to the tissue recovery process, such as rectal mucosal regeneration. Fundamentally, simple approaches such as apoptosis or inflammation have limitations in radiation toxicity assessment. A more appropriate approach is needed in order to reflect all the various factors in the radiation toxicity analysis.

This study had some limitations. First, it was difficult to guarantee that the planned radiation dose was transmitted to the pancreas entirely, due to the respiratory motion in the abdomen. Targeted radiation of the rectum and pancreas by precision small-animal

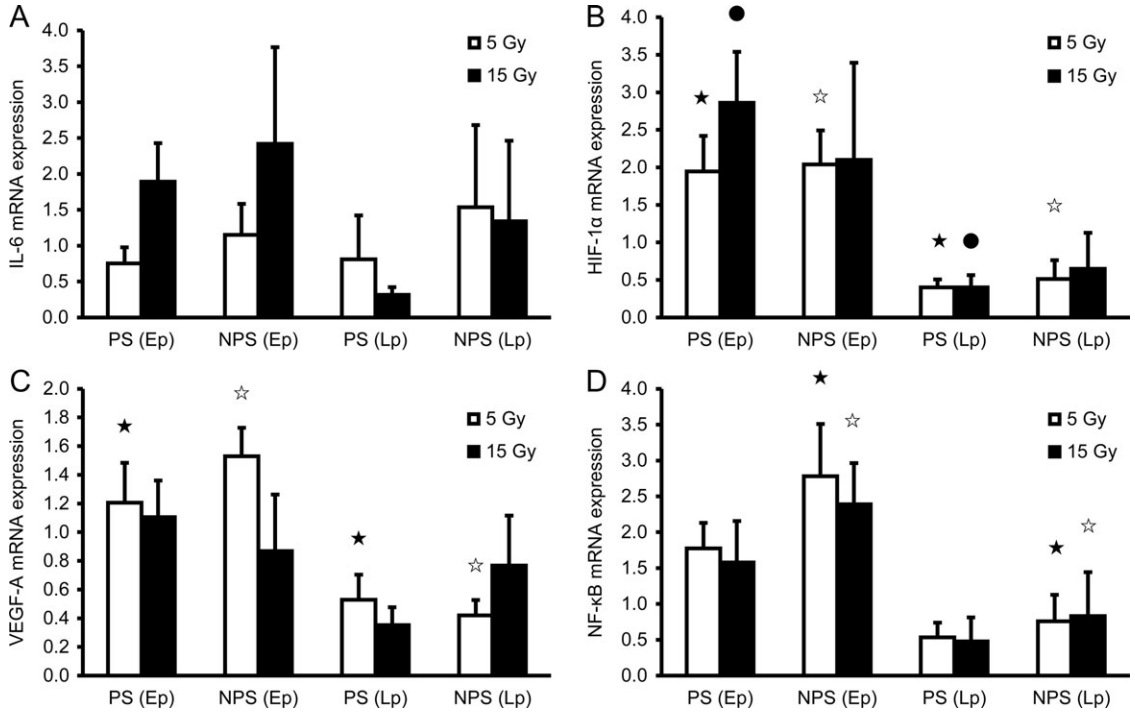

Fig. 7. Relative mRNA expression (real time PCR using rat-specific primers) compared with one control subject at the first week (early phase, Ep) and the 14th week (late phase, Lp) after irradiation for each group. (A) Interleukin-6 (IL-6). (B) Hypoxia-inducible factor (HIF)-1α. (C) Vascular endothelial growth factor (VEGF)-A. (D) Nuclear factor (NF)-κB. Data represent the mean and 95% confidence interval of the results of three independent experiments, each with six samples. A significant Ep–Lp decrease pairs ($P < 0.05$) for the same dose and pancreatic shield condition are denoted as filled stars, empty stars, and filled circles.

irradiation platforms could help to determine more accurately the role of the pancreas in rectal radiation toxicity in future studies. Second, simple approaches such as the AI or CCP3 positivity had limitations in estimating the essential effects of the pancreas in toxicity analysis. More sophisticated data need to be derived through more diversified approaches in the future. Third, totally sham-irradiated controls were not used in the current study. This is because we focused solely on PRE under the precondition of rectal radiation. However, the lack of sham-irradiated controls made it difficult to assess the severity of the rectal radiation toxicity more systematically. A follow-up study will require a more comprehensive approach.

In conclusion, the iCPR method is feasible for assessing the multi-organ effect in the clinical situation-simulating *in vivo* study. PS irradiation is helpful in reducing the negative factors of GIT toxicity from the various perspectives of nutritional status, apoptosis, fibrotic tissue recovery, and inflammation. Above all, it is noteworthy that PS was associated with a tendency toward less toxicity, despite the same rectal dose and more unfavorable dosimetric conditions compared with NPS.

ACKNOWLEDGEMENTS

The authors would like to thank Editage for the English language review. A part of this work was presented at 59th Annual Meeting of the American Society for Radiation Oncology, San Diego, CA, from 24 to 27 September 2017.

CONFLICT OF INTEREST

The authors declare that they have no conflict of interest.

FUNDING

This work was supported by GRANTS from the National Research Foundation (NRF) of Korea [grant numbers NRF-2014R1A1A2058055 and NRF-2016R1D1A1B03935140].

REFERENCES

1. Polistena A, Johnson LB, Ohiami-Masseron S et al. Local radiotherapy of exposed murine small bowel: apoptosis and inflammation. *BMC Surg* 2008;8:1.
2. Nagtegaal ID, Gaspar CG, Peltenburg LT et al. Radiation induces different changes in expression profiles of normal rectal tissue compared with rectal carcinoma. *Virchows Arch* 2005;446:127–35.
3. Bowen JM, Gibson RJ, Keefe DM. Animal models of mucositis: implications for therapy. *J Support Oncol* 2011;9:161–8.
4. Ong ZY, Gibson RJ, Bowen JM et al. Pro-inflammatory cytokines play a key role in the development of radiotherapy-induced gastrointestinal mucositis. *Radiat Oncol* 2010;5:22.

5. Bae BK, Kang MK, Kim JC et al. Simultaneous integrated boost intensity-modulated radiotherapy versus 3-dimensional conformal radiotherapy in preoperative concurrent chemoradiotherapy for locally advanced rectal cancer. *Radiat Oncol J* 2017;35:208–16.
6. Lee DS, Woo JY, Kim JW et al. Re-irradiation of hepatocellular carcinoma: clinical applicability of deformable image registration. *Yonsei Med J* 2016;57:41–9.
7. Ahmadu-Suka F, Gillette EL, Withrow SJ et al. Pathologic response of the pancreas and duodenum to experimental intraoperative irradiation. *Int J Radiat Oncol Biol Phys* 1988;14:1197–204.
8. Zook BC, Bradley EW, Casarett GW et al. Pathologic effects of fractionated fast neutrons or photons on the pancreas, pylorus and duodenum of dogs. *Int J Radiat Oncol Biol Phys* 1983;9:1493–504.
9. Nam H, Lim DH, Kim S et al. A new suggestion for the radiation target volume after a subtotal gastrectomy in patients with stomach cancer. *Int J Radiat Oncol Biol Phys* 2008;71:448–55.
10. Gemici C, Sargin M, Uygur-Bayramicli O et al. Risk of endocrine pancreatic insufficiency in patients receiving adjuvant chemoradiation for resected gastric cancer. *Radiother Oncol* 2013; 107:195–9.
11. Wydmanski J, Polanowski P, Tukiendorf A et al. Radiation-induced injury of the exocrine pancreas after chemoradiotherapy for gastric cancer. *Radiother Oncol* 2016;118:535–9.
12. Kerr JF, Winterford CM, Harmon BV. Apoptosis. Its significance in cancer and cancer therapy. *Cancer* 1994;73:2013–26.
13. Hall PA, Coates PJ, Ansari B et al. Regulation of cell number in the mammalian gastrointestinal tract: the importance of apoptosis. *J Cell Sci* 1994;107(Pt 12):3569–77.
14. Ghobadi G, van der Veen S, Bartelds B et al. Physiological interaction of heart and lung in thoracic irradiation. *Int J Radiat Oncol Biol Phys* 2012;84:e639–46.
15. Wang J, Zheng H, Sung CC et al. The synthetic somatostatin analogue, octreotide, ameliorates acute and delayed intestinal radiation injury. *Int J Radiat Oncol Biol Phys* 1999;45:1289–96.
16. Lloyd-Still JD, Uhing MR, Arango V et al. The effect of intestinal permeability on pancreatic enzyme-induced enteropathy in the rat. *J Pediatr Gastroenterol Nutr* 1998;26:489–95.
17. Kimura RE, Arango V, Lloyd-Still J. Indomethacin and pancreatic enzymes synergistically damage intestine of rats. *Dig Dis Sci* 1998;43:2322–32.
18. Blirando K, Milliat F, Martelly I et al. Mast cells are an essential component of human radiation proctitis and contribute to experimental colorectal damage in mice. *Am J Pathol* 2011;178: 640–51.
19. Kim KT, Chae HS, Kim JS et al. Thalidomide effect in endothelial cell of acute radiation proctitis. *World J Gastroenterol* 2008; 14:4779–83.
20. Berthrong M. Pathologic changes secondary to radiation. *World J Surg* 1986;10:155–70.
21. Sarri Y, Conill C, Verger E et al. Effects of single dose irradiation on pancreatic beta-cell function. *Radiother Oncol* 1991;22:143–4.
22. Langberg CW, Sauer T, Reitan JB et al. Relationship between intestinal fibrosis and histopathologic and morphometric changes in consequential and late radiation enteropathy. *Acta Oncol* 1996;35:81–7.
23. Ferreira MR, Muls A, Dearnaley DP et al. Microbiota and radiation-induced bowel toxicity: lessons from inflammatory bowel disease for the radiation oncologist. *Lancet Oncol* 2014; 15:e139–47.
24. Nakahashi-Oda C, Udayanga KG, Nakamura Y et al. Apoptotic epithelial cells control the abundance of Treg cells at barrier surfaces. *Nat Immunol* 2016;17:441–50.